

## Leading order track functions in a hot and dense QGP

João Barata<sup>\*</sup> and Robert Szafron<sup>†</sup>

*Physics Department, Brookhaven National Laboratory, Upton, New York 11973, USA*



(Received 17 January 2024; accepted 2 July 2024; published 6 August 2024)

We study the modifications to the fragmentation pattern of partons into charged particles in the presence of a hot and dense quark gluon plasma. To this end, we analyze the perturbative renormalization group equations of the track functions, which describe the energy fraction carried by charged hadrons. Focusing on pure Yang-Mills theory, we compute the lowest-order moments of the medium-modified track functions, which are found to be sensitive to the reduced phase space for emissions in the medium and to energy loss. We use the extracted moments to calculate the energy energy correlator (EEC) on tracks in the collinear limit. The EEC on medium-evolved tracks does not differ qualitatively from the EEC on vacuum tracks despite being sensitive to the color decoherence transition and suppressing the distribution due to quenching, as seen in other jet observables.

DOI: [10.1103/PhysRevD.110.L031501](https://doi.org/10.1103/PhysRevD.110.L031501)

**Introduction.** Jets are an ideal tool for studying the time evolution and spatial structure of the quark gluon plasma (QGP) produced in heavy ion collisions. When using jets in this manner, two problems need to be addressed; how the QCD matter modifies the jets' structure [1,2] and which observables best reveal the medium imprints in the measured distributions [3,4].

Regarding the latter point, we address an open question about energy energy correlator (EEC) measurements inside jets, i.e., in the collinear limit, traveling through the QGP [5–10]. The EEC is the simplest correlation function constructed from light-ray operators measuring the asymptotic energy flow passing through idealized calorimeters, see e.g., [11–13]. It can be written in terms of the inclusive two-particle cross section as [14]

$$\frac{d\Sigma^{(n)}}{d\chi} = \sum_{\{i,j\}} \int d\sigma \frac{E_i^n E_j^n}{p_i^{2n}} \delta(\vec{n}_i \cdot \vec{n}_j - \cos \chi), \quad (1)$$

where  $\vec{n}_i$  denotes the spatial direction of the measured energy flow,  $E_i$  is the energy of particle  $i$ ,  $p_i$  is the total energy of the system, and the sum is taken over all particles in the final state. The integer  $n \geq 1$  is introduced as an effective way to further suppress contributions to the EEC from soft emissions.

Values of  $n > 1$  are especially relevant in the heavy ion context where uncorrelated soft sources contaminate jets. In

such cases, the EEC is infrared-and-collinear (IRC) unsafe, and Eq. (1) cannot be evaluated perturbatively. Nonetheless, one can separate the perturbative and nonperturbative contributions to the EEC [12,15]. The matching coefficients between the parton level EEC and the full distribution are given by the moments of the track functions (TFs) [16].<sup>1,2</sup> They satisfy a nonlinear renormalization group (RG) evolution governed by anomalous dimensions, which can be computed in perturbation theory, due to their UV nature.

Several theoretical and phenomenological aspects of the track functions have been explored for pure vacuum evolution, see e.g., [12,15–18]. They have not been studied in the heavy ion context, and the in-medium EEC calculations have neglected the matching to the hadronic level observable [5,9]. This work aims to be the first to analyze medium effects on track functions phenomenologically and explore their impact on jet EEC. To that end, we compute the medium-induced corrections to the TFs' RG structure and the respective anomalous dimensions, which fully relate the moments of the tracks at different momentum scales.

**Leading-order vacuum track functions.** TFs were first introduced a decade ago [16,17], allowing to compute jet observables based on hadrons with specific quantum numbers in a theoretically well-defined way; in particular, TFs allow to compare theory calculations to experimental measurements on charged tracks. A track function  $T_f(x)$  describes the fragmentation of a parton of flavor  $f$  into a

<sup>\*</sup>Contact author: [jlouenco@bnl.gov](mailto:jlouenco@bnl.gov)

<sup>†</sup>Contact author: [rszafron@bnl.gov](mailto:rszafron@bnl.gov)

Published by the American Physical Society under the terms of the [Creative Commons Attribution 4.0 International license](https://creativecommons.org/licenses/by/4.0/). Further distribution of this work must maintain attribution to the author(s) and the published article's title, journal citation, and DOI. Funded by SCOAP<sup>3</sup>.

<sup>1</sup>This issue can also be avoided by defining the EEC on objects which are naturally IRC safe [9].

<sup>2</sup>Other jet observables may require knowing more than the moments of the TFs. We shall not consider these cases, restricting the discussion to the EEC.

subset of hadrons<sup>3</sup> carrying an energy fraction  $x$ . Similarly to collinear fragmentation functions (FFs) [19], TFs are intrinsically nonperturbative. However, unlike FFs, they obey a highly nonlinear RG evolution [15,20,21], more closely related to multihadron fragmentation [22].<sup>4</sup> At leading order (LO) in  $\alpha_s$ ,  $T_i(x)$  satisfies [16,20],

$$\begin{aligned} \mu \frac{dT_i(x, \mu)}{d\mu} &= \sum_{j,k} \int_0^1 dz \frac{\alpha_s}{2\pi} P_{i \rightarrow jk}(z) \\ &\times \int_{x_1, x_2} T_j(x_1, \mu) T_k(x_2, \mu) \delta(x - zx_1 - (1-z)x_2), \end{aligned} \quad (2)$$

where  $P_{i \rightarrow jk}$  are the LO regularized QCD splitting functions [23], and the evolution is expressed in terms of the renormalization scale  $\mu$ , see Fig. 1. The Dokshitzer-Gribov-Lipatov-Altarelli-Parisi (DGLAP) evolution [23–25] can be recovered by restricting Eq. (2) to a one-body evolution, i.e., when it is fully inclusive by replacing  $T_k(x) \rightarrow \delta(x)$  [26], for a subset of particles.<sup>5</sup>

The RG equation simplifies for the track functions' moments<sup>6</sup>

$$T_i^{[N]} \equiv \int_0^1 dz z^N T_i(z). \quad (3)$$

In Yang-Mills (YM) theory, it follows from Eq. (2) that the moments satisfy,

$$\begin{aligned} \mu \frac{dT_i^{[N]}}{d\mu} &= \frac{\alpha_s}{2\pi} \int_0^1 dz P(z) \\ &\times \int_{x_1, x_2} T(x_1, \mu) T(x_2, \mu) (zx_1 + (1-z)x_2)^N, \end{aligned} \quad (4)$$

where  $P(z) \equiv P_{g \rightarrow gg}(z) = 2N_c(z/(1-z)_+ + (1-z)/z + z(1-z)) + 11N_c/6\delta(1-z)$  and  $T(z) = T_g(z)$ . Using conservation of energy to impose the sum rule  $T^{[0]} = 1$ , and the symmetry of the splitting function under the integral after shifting the poles to  $z = 1$ , i.e.,  $\int_z P(z)(1-z) = \int_z P(z)z$ , the leading moments' evolution reads,

$$\begin{aligned} \mu \frac{dT^{[1]}}{d\mu} &= -\frac{\alpha_s}{\pi} \gamma(2) T^{[1]}, \\ \mu \frac{dT^{[2]}}{d\mu} &= -\frac{\alpha_s}{\pi} (\gamma(3) T^{[2]} - (\gamma(2) - \gamma(3)) T^{[1]} T^{[1]}). \end{aligned} \quad (5)$$

The RG of the TFs' moments is fully determined by the anomalous dimensions,

<sup>3</sup>We have in mind the fragmentation into charged hadrons, but the calculation is valid for other conserved quantum numbers.

<sup>4</sup>See [15] for a detailed description of the TFs RG.

<sup>5</sup> $\int_x$  denotes the phase space integral in the energy fraction  $x$ .

<sup>6</sup>The dependence in  $\mu$  is made implicit.

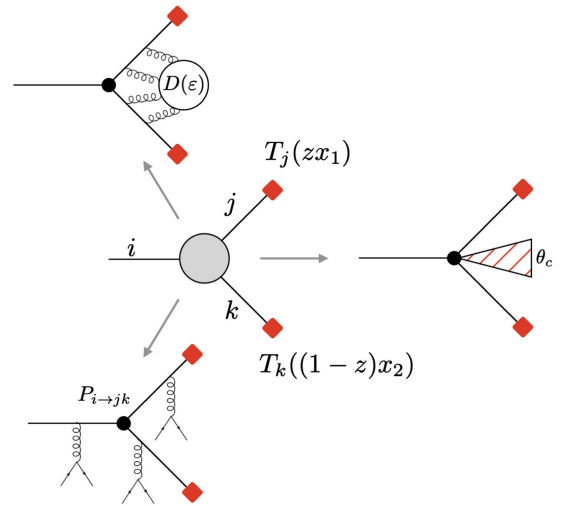


FIG. 1. Diagrammatic representation of the LO evolution [see Eq. (2)] and the different medium modifications we take into account; energy loss (top left), induced radiation (bottom left), and reduced phase space (right).

$$\gamma(j) \equiv - \int_0^1 dz z^{j-1} P(z), \quad (6)$$

where in the vacuum  $\gamma_{\text{vac}}(j) = -11N_c/6 - 2N_c[(1/(j^2 - j) + 1/((j+1)(j+2)) - \psi(j+1) - \gamma_E]$ , with  $\psi(j) \equiv \Gamma'(j)/\Gamma(j)$  the digamma function and  $\gamma_E \approx 0.577$  the Euler-Mascheroni constant. Equation (5) can be simplified in YM theory, where  $\gamma(2) = 0$ . This sum rule is derived from energy conservation. It imposes a nonperturbative constraint that also applies to in-medium evolution, provided that energy loss effects are absent. The related RG invariance under the shift symmetry  $T(x) \rightarrow T(x+b)$  [15,20] constrains higher moments' evolution, but there are no further nontrivial constraints in YM theory. Below, we compute the medium modifications to Eq. (5), which can typically be absorbed into a redefinition of  $\gamma(j)$ . We later discuss how these modifications affect the EEC on tracks.

*Medium modifications to the track functions.* We assume that the partonic cascade occurs in a homogeneous and isotropic gluonic QCD medium, with a sizeable longitudinal extension  $L$ .<sup>7</sup> We take the interactions with the underlying matter to be dominated by multiple soft gluon exchanges, see Fig. 1, which are captured in the Baier-Dokshitzer-Mueller-Peigne-Schiff-Zakharov/Armesto, Salgado Wiedemann (BDMPS-Z/ASW) phenomenological model [30–33]. Large momentum exchanges with the medium are neglected; the discussion can be easily extended to such cases.

We first consider the hardest branchings in the cascade, which are primarily vacuumlike [34]. The phase space for these emissions, at leading logarithmic accuracy, can be captured by the formation time  $t_f = 2/(z(1-z)\theta^2 p_t)$ ; the

<sup>7</sup>For recent developments in describing fragmentation in more realistic matter models see e.g., [27–29].

radiation pattern is modified depending on the ordering of  $t_f$  with respect to the characteristic timescale generated by the medium,  $t_c$ . The vacuumlike region corresponds to  $t_f < t_c$  [34]. The vacuumlike sector is also defined by  $\theta > \theta_c$ , where  $\theta_c$  is the characteristic medium angular scale. For the matter model considered, the characteristic angular scale is  $\theta_c \equiv 2/\sqrt{\hat{q}_{\text{eff}}L^3}$  [35,36], with  $\hat{q}_{\text{eff}} = \hat{q}(1-z+z^2) \equiv \hat{q}f(z)$  the effective jet quenching transport coefficient in YM theory, and  $\hat{q}$  is the scalar adjoint transport coefficient; the corresponding characteristic time scale is  $t_c = \sqrt{2z(1-z)p_t/\hat{q}_{\text{eff}}}$  [34,37]. This leading logarithmic parametrization of the phase space for the virtuality cascade naively extends the double logarithmic construction introduced in [34]. Thus, it should only be understood as a physically motivated model for describing the vacuum cascade in the medium; other models can be found in the literature [38–40].

We consider two different phase spaces for vacuum emission, differing mainly in the inclusion of out-of-the-medium fragmentation. Since the cascade still obeys vacuum evolution, the functional form of Eq. (4) is not affected, and the phase space modification can be formally absorbed into the anomalous dimension [9,34],<sup>8</sup>

$$\gamma(j, \mu) = - \int_0^1 dz P(z) \Theta_{\text{PS}}(\mu, z) z^{j-1}, \quad (7)$$

where  $\Theta_{\text{PS}}$  denotes the allowed phase space for fragmentation. The first model only allows for branchings to occur if they are sufficiently short-lived and wide-angled to be resolved [37];  $\Theta_{\text{PS}}^{(1)} = \Theta(\mu - p_t \theta_c) \Theta(t_c - t_f)$ , where the scale  $\mu = p_t \theta$ . The second phase space we study allows fragmentation in the region  $t_f > L$  [34]:  $\Theta_{\text{PS}}^{(2)} = 1 - \Theta(t_f - t_c) \Theta(L - t_f)$ . Both phase spaces are formally only well-described in the  $z \ll 1$  limit, but we naively extend them to full kinematics. A study of the phase space structure at finite energy fractions is still missing from the literature.

We first compute the anomalous dimensions in the soft limit to understand the medium modifications better. Using the soft Balitsky-Fadin-Kuraev-Lipatov (BFKL) form of the vacuum anomalous dimension,  $\gamma_{\text{vac}}^{\text{BFKL}}(j) = \frac{2N_c}{1-j}$ , we find that,

$$\gamma^{(i)}(j, \mu) = \gamma_{\text{vac}}^{\text{BFKL}}(j) (\lambda_{i+}^{j-1} - \lambda_{i-}^{j-1} + \delta_{i,2}), \quad (8)$$

where  $i = 1, 2$  denotes the phase space model,  $\lambda_{1-} = \lambda_{2+} = \sqrt[3]{2\hat{q}p_t/\mu^4}$ ,  $\lambda_{1+} = 1$ ,  $\lambda_{2-} = 2p_t/(\mu^2L)$ , and the phase space constraints depending only on  $\mu$  are left implicit. The BFKL pole vanishes inside the medium since soft gluons cannot go on shell. Equation (8) ensures the strongest medium modifications occur at smaller integer

<sup>8</sup>This modification is tied to the particular medium model employed.

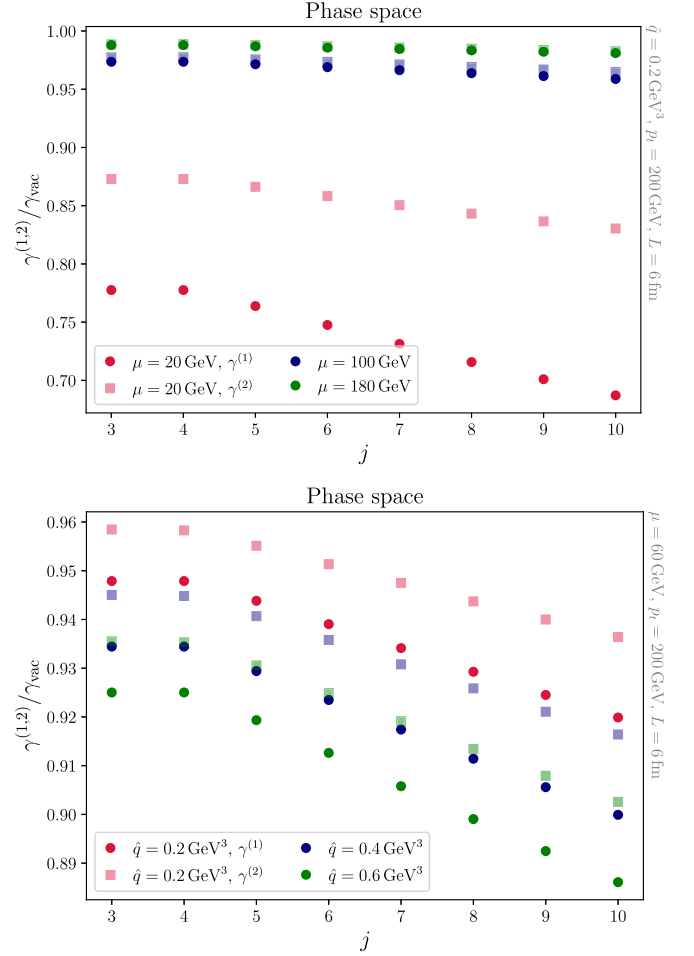


FIG. 2. Anomalous dimensions' evolution as a function of  $\mu$  and the jet quenching parameter  $\hat{q}$ . Ratios smaller than unity will result in a suppression of the EEC.

values  $j > 1$ . In what follows, all numerical results are obtained without using the soft limit.

In Fig. 2, we show the anomalous dimensions for both models at finite  $z$  while imposing the sum rule  $\gamma(2) = 0$ , taking the ratio to the vacuum result. Values in the y-axis smaller than unity indicate a deceleration in the RG evolution; the  $\gamma \rightarrow 0$  limit freezes the evolution. At the EEC level, the larger the difference to the vacuum, the more suppressed the observable is, as illustrated below. On top, we show the evolution with the scale  $\mu$ . As expected, if  $\mu \approx p_t$  (i.e.,  $\theta \approx 1$ ), we recover the vacuum result as there is no loss of phase space, i.e., energetic jets are not sensitive to the medium. Taking the evolution scale down, the medium reduces the phase space available to radiate, and the anomalous dimension decreases. The significant difference between the two models resides in the  $\mu \rightarrow 0$  region (at fixed  $p_t$ ); while  $\gamma^{(1)} \rightarrow 0$ ,  $\gamma^{(2)} \rightarrow \gamma_{\text{vac}}$  since at small angles out-of-the-medium emissions are included, see Fig. 3 in [9]. At fixed  $\mu$ , the denser the medium, the larger the modification, as expected. These are more prominent for  $\gamma^{(1)}$ , where no out-of-the-medium evolution is incorporated, and for larger  $j$ .

The latter originate from intermediate values of  $z$ , explaining the difference to the soft limit.

As illustrated in Fig. 1, in-medium evolution also produces bremsstrahlung radiation parallel to the virtuality cascade. This mechanism has two significant phenomenological consequences; the enhancement of the splitting function at large angles and radiative energy loss to the matter. We describe how these effects can be incorporated into the evolution of the TFs.

The multiple soft momentum gluons exchanged with the medium result in a characteristic interference pattern, leading to the enhanced Landau—Pomeranchuk—Migdal branching rate [41–43]. This regime, captured in the BDMPS-ASW approximation, is valid for intermediate energies of the radiated partons,  $\omega_{\text{BH}} < z(1-z)p_t < \omega_c$ , where  $\omega_{\text{BH}}$  denotes the Bethe-Heitler frequency, below which the radiative spectrum is dominated by incoherent contributions [44], and  $\omega_c = \frac{1}{2}\hat{q}L^2$  denotes the characteristic frequency above which the gluon resolves the medium coherently. A closed form for the radiation rate is not known in QCD in this region of phase space; we consider an asymptotic limit of exactly collinear branchings followed by in-medium diffusion,<sup>9</sup>

$$\frac{dI}{dzd\mu z^2(1-z)^2\mu} = \int_0^L dt \frac{\mathcal{P}(\mu z(1-z), L-t)}{2\pi} \frac{dI}{dzdt}, \quad (9)$$

where  $dI/dzdt$  denotes the induced radiation rate and  $\mathcal{P}$  is the momentum broadening distribution. Transverse momentum is only acquired due to the evolution between the time the outgoing states go on shell and the end of the medium; the in-medium rate determines the energy distribution. In the BDMPS-Z/ASW approximation the broadening distribution is purely diffusive [46,47],  $\mathcal{P}(k, t) = 4\pi/(\hat{q}_{\text{eff}}t) \exp(-k^2/(\hat{q}_{\text{eff}}t))$ ; the radiative rate reads [46,48],

$$\frac{dI}{dzdt} = \frac{\alpha_s N_c}{2\pi} \frac{f^{\frac{3}{2}}(z)}{(z(1-z))^{\frac{3}{2}}} \sqrt{\frac{\hat{q}}{p_t}}. \quad (10)$$

Equation (10) can be regularized by a plus distribution while shifting the singularities to  $z = 1$ , and using the integral identity [46],

$$\int_{\epsilon}^{1-\epsilon} dz \frac{dI}{dzdt} = \int_0^{1-\epsilon} dz 2z \frac{dI}{dzdt}. \quad (11)$$

Combining all elements, Eq. (9) becomes

$$\frac{dI}{dzd\mu} = \frac{\alpha_s N_c}{\pi} \sqrt{\frac{1}{\hat{q}p_t}} \mu \frac{(2z)z^2(1-z)^2 f^{\frac{3}{2}}(z)}{(z(1-z))^{\frac{3}{2}}} \Gamma_0 \left( \frac{z^2(1-z)^2 \mu^2}{f(z)\hat{q}L} \right), \quad (12)$$

where  $\Gamma_0$  denotes the incomplete gamma function.

We include the medium-induced kernel in the splitting functions entering the RG evolution in Eq. (4). Such a choice has been applied in different jet quenching phenomenological studies, see [38,40,49–51]. Note that the in-medium effects impact both the operators' anomalous dimensions and matrix elements, i.e., the boundary conditions for the evolution. We start the evolution from the hard scale, where the in-medium effects can be treated perturbatively. Thus, in an effective field theory spirit, the hard scale is assumed to be parametrically much larger than medium-induced scales, and the dominant effect comes from the evolution, i.e., from in-medium modification of the anomalous dimensions. A complete effective field theory formulation of in-medium effects is missing; although such an effort would be worthwhile, it goes past the current scope, and we leave it for future work. The anomalous dimensions in Eq. (6) become

$$\begin{aligned} \gamma(j, \mu) = & - \int_0^1 \left\{ P(z) + N_c \mu^2 \sqrt{\frac{1}{\hat{q}p_t}} \right. \\ & \left. \times 2z \sqrt{z(1-z)} f^{\frac{3}{2}}(z) \Gamma_0 \left( \frac{z^2(1-z)^2 \mu^2}{f(z)\hat{q}L} \right) \right\} z^{j-1}, \quad (13) \end{aligned}$$

up to a  $\delta(z-1)$  term, whose coefficient can be obtained by imposing the sum rule  $\gamma(2) = 0$ . In Fig. 3 we evaluate Eq. (13). To ensure that the collinear cascade approximation is valid, we require  $p_t \ll \hat{q}L^2$  [48]; thus, we use small  $p_t$ , which should be thought as the energy of the emitter. Too large energies will break the collinear cascade approximation, resulting in unphysical values of anomalous dimensions. Therefore, we take a long medium with  $L = 10$  fm and a small jet energy with  $p_t = 15$  GeV. The results show a mild dependence on  $j$ , while the evolution in  $\mu$  is fast, leading to a substantial enhancement that competes with the phase space constraint effect in Fig. 2. The magnitude of the increase is related to the asymptotic approximation used, although other calculations of the in-medium rate at finite  $z$  exist [52–56], it is unclear how to incorporate them in the RG evolution at present.<sup>10</sup> Due to the high sensitivity to the modeling, we will not discuss these contributions further; nonetheless, we expect this modification to yield a small effect due to the absence of a collinear pole in the medium. Incorporating the modified splitting function in this manner, the growth of the anomalous dimensions needs to be tamed by introducing coherence effects; see [35,58].

<sup>9</sup>See e.g., [45] for further discussion on this approximation.

<sup>10</sup>This is possible for dilute matter [57].

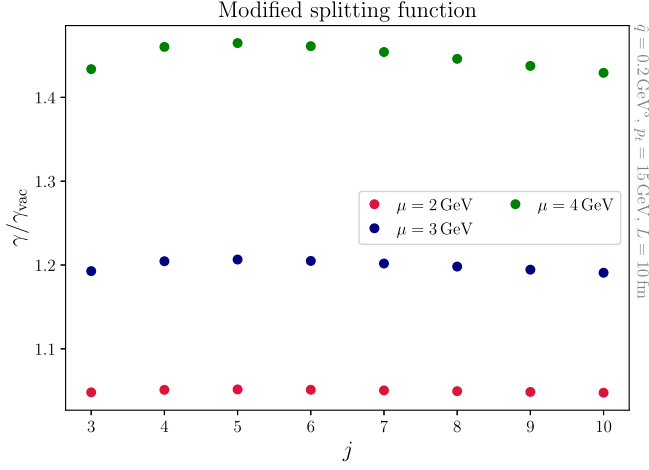


FIG. 3. Anomalous dimension's evolution including medium induced radiation. Since the ratio is larger than unity, this modification will result in an enhancement of the EEC.

So far, we have considered the contribution of bremsstrahlung radiation, which hadronizes into charged hadrons. However, a substantial part of the softer induced radiation feeds down to the medium scale, and it should be viewed as part of the QGP, quenching the jet energy. We describe these lost emissions in terms of a distribution function  $D(\varepsilon)$ , with  $\varepsilon \ll p_t$  representing the amount of quenched energy, see Fig. 1. This distribution can be computed perturbatively under certain limits [32,59,60], but it is expected to have a significant nonperturbative contribution. Therefore, we remain agnostic to its functional form and only impose overall energy conservation,  $\int_0^\infty d\varepsilon D(\varepsilon) = 1$ .

To implement the effect of energy loss in the TFs' RG, we first consider DGLAP evolution; at  $\mathcal{O}(\alpha_s^2)$  the real contribution to the gluon distribution  $G$  reads [23],

$$G(x, \mu)|_{\text{real}}^{\mathcal{O}(\alpha_s^2)} = \frac{\alpha_s^2}{(2\pi)^2} \int_{z_1, z_2, x_1} \hat{P}(z_1) \hat{P}(z_2) \times \int_{\mu_0}^{\mu} d \ln \mu' \int_{\mu_0}^{\mu'} d \ln \mu'' G(x_1, \mu'') \times \delta(x - x_1 z_1 (1 - z_2)), \quad (14)$$

where  $\hat{P}(z) = \hat{P}(1 - z)$  is the unregularized splitting function. We choose  $z_2$  to represent the fraction of energy lost to the matter. The rhs of Eq. (14) can be simplified (dropping the  $\mu$  dependence),

$$\frac{\alpha_s^2}{(2\pi)^2} \int_x^1 dz_1 \int_0^{1-\frac{x}{z_1}} dz_2 \frac{\hat{P}(z_1) \hat{P}(z_2)}{z_1(1-z_2)} G\left(\frac{x}{z_1(1-z_2)}\right) \approx \frac{\alpha_s}{2\pi} \int_x^1 \frac{dz_1}{z_1} \int_0^{(z_1-x)p_t} d\varepsilon \hat{P}\left(z_1 + \frac{\varepsilon}{p_t}\right) D(\varepsilon) G\left(\frac{x}{z_1}\right), \quad (15)$$

where we replaced the second splitting function by the energy loss distribution  $D(\varepsilon)$ , modeling energy transferred to the matter, see Fig. 1. Assuming  $1 > x \sim z_1 \gg \frac{\varepsilon}{p_t}$ , the

upper cutoff of the  $\varepsilon$  integration should be extended to infinity. Treating the energy loss as an additional convolution within the standard DGLAP cascade and including the virtual corrections, we find

$$\mu \frac{dG(x, \mu)}{d\mu} \approx \frac{\alpha_s}{2\pi} \int_{x_1, z} \int_0^\infty d\varepsilon D(\varepsilon) P\left(z + \frac{\varepsilon}{p_t}\right) \times G(x_1) \delta(x - x_1 z), \quad (16)$$

which agrees with the Sudakov factor in [60]. A similar procedure for the TFs, with the initial truncation in Eq. (14) at  $\mathcal{O}(\alpha_s^3)$ , with  $\delta(x - x_1 z (1 - z_2)) \rightarrow \delta(x - x_1 z_1 (1 - z_2) - x_2 (1 - z_1) (1 - z_3))$ , where  $z_2, z_3$  are the energy loss fractions from uncorrelated emissions, leads to

$$\mu \frac{dT}{d\mu} = \frac{\alpha_s}{2\pi} \int_{\varepsilon_1, \varepsilon_2} D(\varepsilon_1) D(\varepsilon_2) \int_0^1 dz P\left(z + \frac{\varepsilon_1}{p_t} + \frac{\varepsilon_2}{p_t}\right) \times \int_{x_1, x_2} T(x_1, \mu) T(x_2, \mu) \delta(x - z x_1 - (1 - z) x_2). \quad (17)$$

The upper limit of the  $\varepsilon_{1,2}$  integrals is set to infinity. The evolution for the moments at LO is unchanged with respect to Eq. (4) if the anomalous dimensions include the double convolution with the energy loss probabilities.

Without specifying the form for  $D(\varepsilon)$ , but assuming the energy loss distribution has a small dispersion, we simplify the evolution equation replacing  $\varepsilon$  by its mean value  $\langle \varepsilon \rangle \sim \hat{q} L^2$ . This approximation might be insufficient for phenomenological applications, see e.g. [61]. With this caveat, the anomalous dimension reduces to

$$\gamma(j) = - \int_{\frac{2\langle \varepsilon \rangle}{p_t}}^1 dz P(z) \left(z - \frac{2\langle \varepsilon \rangle}{p_t}\right)^{j-1}, \quad (18)$$

up to a  $\delta(1 - z)$  term ( $\gamma$  is  $\mu$  independent in this case due to the single logarithmic structure of the expansion). We can

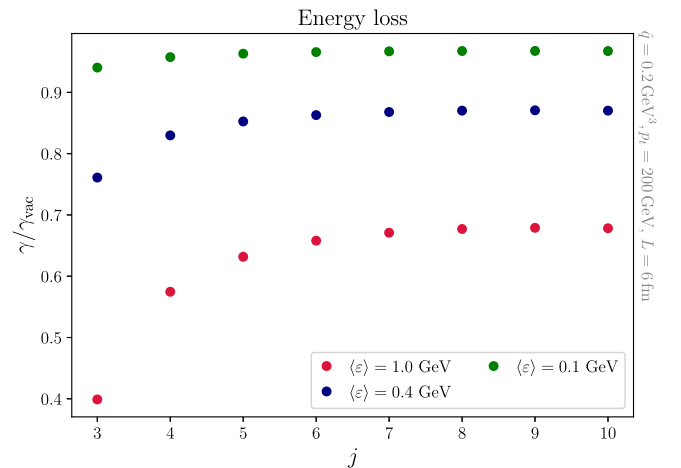


FIG. 4. Anomalous dimension evolution including average energy loss effects. We use the same parameters as in Fig. 2.

no longer fix its coefficient via the sum rule  $\gamma(2) = 0$  since we assumed  $1 > x \gg \frac{\epsilon}{p_t}$ . Nonetheless, we impose the sum rule in Fig. 4 to directly compare energy-loss driven modifications to Figs. 2 and 3; this results in an overall shift, with minimal modifications to the shape. Compared to the naive estimation from the BDMPS-Z/ASW approximation,  $\langle \epsilon \rangle_{\text{BDMPS-Z/ASW}} \sim \mathcal{O}(20)$  GeV, we observe significant effects already for  $\langle \epsilon \rangle$  one order of magnitude lower (red markers). This is likely due to the mean value approximation, which typically overestimates the quenching effects [61]. Consequently, to avoid nonphysical results, we restrict ourselves to small values for  $\langle \epsilon \rangle / p_t$ .

*Application to EECs.* Having considered the modifications to the TFs' RG evolution, we study their impact on the EEC. The LO EEC on tracks is defined as [12,15]

$$\begin{aligned} \frac{d\Sigma_{\text{trk}}^{(n)}}{d\chi} &\equiv \int_{z, x_1, x_2} x_1^n T(x_1) x_2^n T(x_2) z^n (1-z)^n \frac{d\sigma}{\sigma dz d\chi} \\ &= \int_z T^{[n]}(\chi p_t) T^{[n]}(\chi p_t) z^n (1-z)^n \frac{d\sigma}{\sigma dz d\chi}, \end{aligned} \quad (19)$$

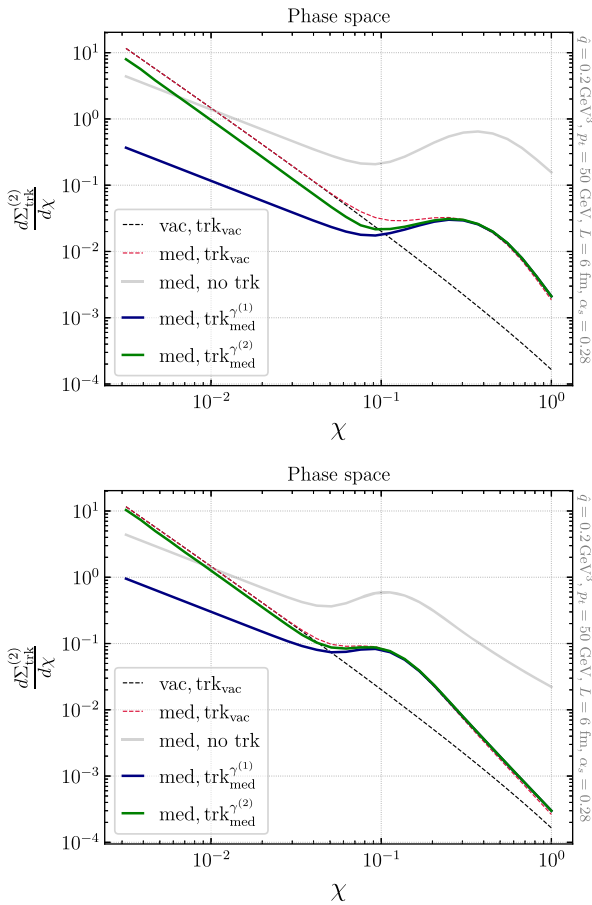


FIG. 5. EEC with  $n = 2$ , including phase space effects. Top:  $p_t = 50$  GeV; Bottom:  $p_t = 200$  GeV.

where we only include terms for  $\chi > 0$ . In YM theory, the lowest order nontrivial track function appears at  $n = 2$ ; see Eq. (5), which we consider in what follows. We work at fixed coupling, such that we are only sensitive to the evolution of the track functions, and for the initial condition, we take the form  $T(x, \mu_0) = 252x^2(1-x)^6$  at  $\mu_0 = p_t$  [17]. Equation (19) is computed using the in-medium cross section obtained in the limit of energetic final states, see [52–54] for details. Writing  $d\sigma = d\sigma_{\text{vac}}(1 + F_{\text{med}})$ , we have

$$\begin{aligned} F_{\text{med}} &= \frac{2}{t_f} \left\{ \int_0^L dt \int_t^L \frac{dt'}{t_f} \left[ \cos\left(\frac{t'-t}{t_f}\right) \mathcal{C}_3(t', t) \mathcal{C}_4(L, t') \right] \right. \\ &\quad \left. - \sin\left(\frac{L-t}{t_f}\right) \mathcal{C}_3(L, t) \right\}. \end{aligned} \quad (20)$$

The correlators  $\mathcal{C}_{3,4}$  in the BDMPS-Z/ASW approximation take the form  $\mathcal{C}_3(t', t) \approx e^{-\frac{1}{12}\hat{q}\chi^2(t'-t)^3}$  and  $\mathcal{C}_4(L, t') \approx e^{-\frac{1}{4}\hat{q}\chi^2(L-t')(t'-t)^2}$ , where we neglected the  $z$  dependence in the phases.

The results for  $\Sigma_{\text{trk}}^{(2)}$  are shown in Figs. 5 and 6, where the vacuum and medium modified LO EEC (following [6,9]) on the vacuum evolved TFs are shown by the dashed black

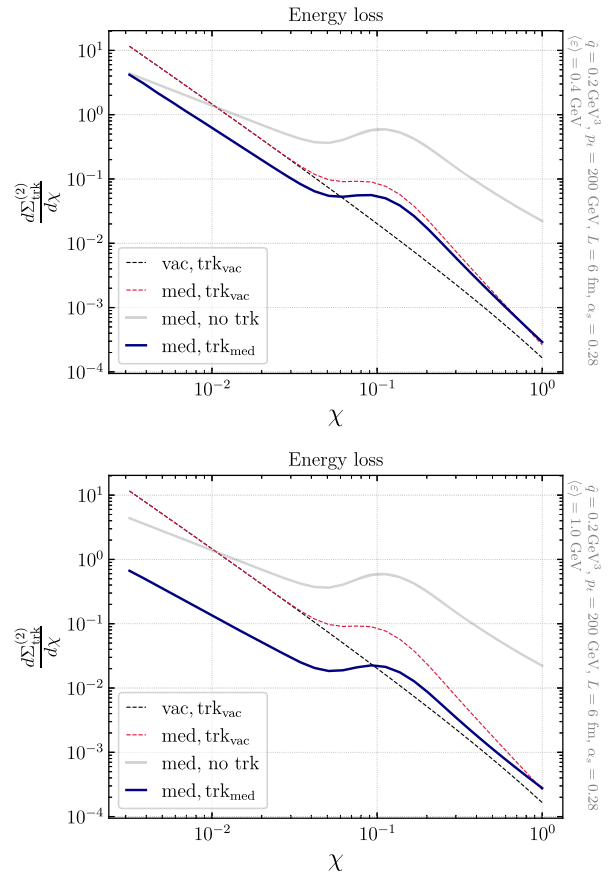


FIG. 6. EEC with  $n = 2$ , including mean energy loss. Top:  $\langle \epsilon \rangle = 0.4$  GeV, Bottom:  $\langle \epsilon \rangle = 1$  GeV.

and red, respectively. The overall normalization is not essential for the current discussion, and it differs from particle-based EECs due to the inclusion of the tracks. In-medium results on medium-evolved TFs are shown by solid lines for the different models. For the case of reduced phase space, including the medium-modified track functions leads to small changes compared to vacuum TFs. The major differences arise at smaller values of  $p_t$ , in the region where the medium leads to an enhancement of the EEC. Significantly, including the in-medium tracks does not alter the shape of the distribution, which allows us to qualitatively visualize the color decoherence transition. The distinction between the phase space models is evident for small  $\chi$ , where out-of-the-medium fragmentation becomes crucial. Mean energy loss shifts the distribution below the vacuum case, as is typical of energy loss effects in jet observables. The overall shape of the distribution is only barely modified, even for the largest  $\langle \epsilon \rangle$ .

*Conclusions.* We conducted the first study of the TFs RG evolution in a dense QGP. Comprehending such effects is vital in heavy ions, where soft, uncorrelated sources

contaminate the jet EEC. We showed that, at a qualitative level, it is adequate to use the vacuum TFs as the QGP medium does not drastically impact the shape of the EEC distribution through the modified TFs.

Our analysis is phenomenologically driven and faces several shortcomings, such as the need to describe the phase space for vacuum-like emissions at leading logarithmic accuracy and the lack of suitable treatment of the in-medium matrix elements. From a phenomenological point of view, it would be worthwhile to extract the in-medium TFs from available data or MC samples. We hope to address these aspects in the future.

*Acknowledgments.* J. B. and R. S. are supported by the United States Department of Energy under Grant Contract No. DESC0012704. We are grateful to Swagato Mukherjee, Guilherme Milhano, Yacine Mehtar-Tani, Ian Moulton, Wenqing Fan, Andrey Sadofyev, Xin-Nian Wang, and Mateusz Ploskon for discussions. We particularly thank Paul Caucal, Pier Monni, and Alba Soto-Ontoso for their collaborative efforts on closely related work and helpful discussions.

- 
- [1] Y. Mehtar-Tani, J. G. Milhano, and K. Tywoniuk, *Int. J. Mod. Phys. A* **28**, 1340013 (2013).
  - [2] G.-Y. Qin and X.-N. Wang, *Int. J. Mod. Phys. E* **24**, 1530014 (2015).
  - [3] L. Cunqueiro and A. M. Sickles, *Prog. Part. Nucl. Phys.* **124**, 103940 (2022).
  - [4] L. Apolinário, Y.-J. Lee, and M. Winn, *Prog. Part. Nucl. Phys.* **127**, 103990 (2022).
  - [5] C. Andres, F. Dominguez, J. Holguin, C. Marquet, and I. Moulton, *J. High Energy Phys.* **09** (2023) 088.
  - [6] C. Andres, F. Dominguez, R. Kunawalkam Elayavalli, J. Holguin, C. Marquet, and I. Moulton, *Phys. Rev. Lett.* **130**, 262301 (2023).
  - [7] J. Barata, J. G. Milhano, and A. V. Sadofyev, *Eur. Phys. J. C* **84**, 174 (2024).
  - [8] J. Barata and Y. Mehtar-Tani, in *11th International Conference on Hard and Electromagnetic Probes of High-Energy Nuclear Collisions: Hard Probes 2023* (2023), arXiv: 2307.08943.
  - [9] J. Barata, P. Caucal, A. Soto-Ontoso, and R. Szafron, arXiv: 2312.12527.
  - [10] Z. Yang, Y. He, I. Moulton, and X.-N. Wang, *Phys. Rev. Lett.* **132**, 011901 (2024).
  - [11] H. Chen, *J. High Energy Phys.* **01** (2024) 035.
  - [12] H. Chen, I. Moulton, X. Zhang, and H. X. Zhu, *Phys. Rev. D* **102**, 054012 (2020).
  - [13] D. M. Hofman and J. Maldacena, *J. High Energy Phys.* **05** (2008) 012.
  - [14] C. L. Basham, L. S. Brown, S. D. Ellis, and S. T. Love, *Phys. Rev. D* **17**, 2298 (1978).
  - [15] Y. Li, I. Moulton, S. S. van Velzen, W. J. Waalewijn, and H. X. Zhu, *Phys. Rev. Lett.* **128**, 182001 (2022).
  - [16] H.-M. Chang, M. Procura, J. Thaler, and W. J. Waalewijn, *Phys. Rev. Lett.* **111**, 102002 (2013).
  - [17] H.-M. Chang, M. Procura, J. Thaler, and W. J. Waalewijn, *Phys. Rev. D* **88**, 034030 (2013).
  - [18] K. Lee and I. Moulton, arXiv:2308.00746.
  - [19] J. C. Collins and D. E. Soper, *Nucl. Phys.* **B194**, 445 (1982).
  - [20] M. Jaarsma, Y. Li, I. Moulton, W. Waalewijn, and H. X. Zhu, *J. High Energy Phys.* **06** (2022) 139.
  - [21] H. Chen, M. Jaarsma, Y. Li, I. Moulton, W. J. Waalewijn, and H. X. Zhu, arXiv:2210.10061.
  - [22] U. P. Sukhatme and K. E. Lassila, *Phys. Rev. D* **22**, 1184 (1980).
  - [23] G. Altarelli and G. Parisi, *Nucl. Phys.* **B126**, 298 (1977).
  - [24] Y. L. Dokshitzer, *Sov. Phys. JETP* **46**, 641 (1977).
  - [25] V. N. Gribov and L. N. Lipatov, *Sov. J. Nucl. Phys.* **15**, 438 (1972).
  - [26] H. Chen, M. Jaarsma, Y. Li, I. Moulton, W. J. Waalewijn, and H. X. Zhu, *J. High Energy Phys.* **07** (2023) 185.
  - [27] A. V. Sadofyev, M. D. Sievert, and I. Vitev, *Phys. Rev. D* **104**, 094044 (2021).
  - [28] M. V. Kuzmin, X. Mayo López, J. Reiten, and A. V. Sadofyev, *Phys. Rev. D* **109**, 014036 (2024).
  - [29] J. Barata, X. Mayo López, A. V. Sadofyev, and C. A. Salgado, *Phys. Rev. D* **108**, 034018 (2023).

- [30] B. G. Zakharov, *JETP Lett.* **63**, 952 (1996).
- [31] U. A. Wiedemann and M. Gyulassy, *Nucl. Phys.* **B560**, 345 (1999).
- [32] R. Baier, Y. L. Dokshitzer, S. Peigne, and D. Schiff, *Phys. Lett. B* **345**, 277 (1995).
- [33] C. A. Salgado and U. A. Wiedemann, *Phys. Rev. D* **68**, 014008 (2003).
- [34] P. Caucal, E. Iancu, A. H. Mueller, and G. Soyez, *Phys. Rev. Lett.* **120**, 232001 (2018).
- [35] J. Casalderrey-Solana, Y. Mehtar-Tani, C. A. Salgado, and K. Tywoniuk, *Phys. Lett. B* **725**, 357 (2013).
- [36] Y. Mehtar-Tani, C. A. Salgado, and K. Tywoniuk, *J. High Energy Phys.* **10** (2012) 197.
- [37] Y. Mehtar-Tani and K. Tywoniuk, *Phys. Rev. D* **98**, 051501 (2018).
- [38] A. Majumder, *Phys. Rev. C* **88**, 014909 (2013).
- [39] K. Zapp, G. Ingelman, J. Rathsman, J. Stachel, and U. A. Wiedemann, *Eur. Phys. J. C* **60**, 617 (2009).
- [40] N. Armesto, L. Cunqueiro, and C. A. Salgado, *Eur. Phys. J. C* **63**, 679 (2009).
- [41] L. D. Landau and I. Pomeranchuk, *Dokl. Akad. Nauk Ser. Fiz.* **92**, 535 (1953).
- [42] A. B. Migdal, *Phys. Rev.* **103**, 1811 (1956).
- [43] S. R. Klein *et al.*, *AIP Conf. Proc.* **302**, 172 (1994).
- [44] H. Bethe and W. Heitler, *Proc. R. Soc. A* **146**, 83 (1934).
- [45] J. Barata, Y. Mehtar-Tani, A. Soto-Ontoso, and K. Tywoniuk, *J. High Energy Phys.* **09** (2021) 153.
- [46] J.-P. Blaizot, F. Dominguez, E. Iancu, and Y. Mehtar-Tani, *J. High Energy Phys.* **06** (2014) 075.
- [47] J. Barata, Y. Mehtar-Tani, A. Soto-Ontoso, and K. Tywoniuk, *Phys. Rev. D* **104**, 054047 (2021).
- [48] J.-P. Blaizot, E. Iancu, and Y. Mehtar-Tani, *Phys. Rev. Lett.* **111**, 052001 (2013).
- [49] W. Ke and I. Vitev, *Phys. Lett. B* **854**, 138751 (2024).
- [50] W.-t. Deng and X.-N. Wang, *Phys. Rev. C* **81**, 024902 (2010).
- [51] Y.-T. Chien, A. Emerman, Z.-B. Kang, G. Ovanessian, and I. Vitev, *Phys. Rev. D* **93**, 074030 (2016).
- [52] J. H. Isaksen and K. Tywoniuk, *J. High Energy Phys.* **11** (2020) 125.
- [53] J. H. Isaksen and K. Tywoniuk, *J. High Energy Phys.* **09** (2023) 049.
- [54] F. Domínguez, J. G. Milhano, C. A. Salgado, K. Tywoniuk, and V. Vila, *Eur. Phys. J. C* **80**, 11 (2020).
- [55] L. Apolinário, N. Armesto, J. G. Milhano, and C. A. Salgado, *J. High Energy Phys.* **02** (2015) 119.
- [56] J.-P. Blaizot, F. Dominguez, E. Iancu, and Y. Mehtar-Tani, *J. High Energy Phys.* **01** (2013) 143.
- [57] M. D. Sievert and I. Vitev, *Phys. Rev. D* **98**, 094010 (2018).
- [58] S. Cao *et al.* (JETSCAPE Collaboration), *Phys. Rev. C* **96**, 024909 (2017).
- [59] Y. Mehtar-Tani and K. Tywoniuk, *Nucl. Phys.* **A979**, 165 (2018).
- [60] Y. Mehtar-Tani and K. Tywoniuk, *J. High Energy Phys.* **04** (2017) 125.
- [61] R. Baier, Y. L. Dokshitzer, A. H. Mueller, and D. Schiff, *J. High Energy Phys.* **09** (2001) 033.